

Communication

Facile Synthesis of Polyacrylic Acid/Graphene Oxide Composite Hydrogel Electrolyte for High-Performance Flexible Supercapacitors

Yue Xin, Zhaoxin Yu, Razium Ali Soomro  and Ning Sun *

Beijing Key Laboratory of Electrochemical Process and Technology for Materials, College of Materials Science & Engineering, Beijing University of Chemical Technology, Beijing 100029, China

* Correspondence: ningsun@mail.buct.edu.cn

Abstract: The development of hydrogel electrolytes plays a critical role in high-performance flexible supercapacitor devices. Herein, a composite hydrogel electrolyte of polyacrylic acid (PAA) and graphene oxide (GO) has been successfully prepared, where the oxygen-containing functional groups of GO may crosslink and form hydrogen bonds with carboxyl on the molecular chain of PAA, thereby significantly enhancing the mechanical properties of a PAA-based gel electrolyte. The tensile strength increases from 4.0 MPa for pristine PAA gel to 6.1 MPa for PAA/GO composite gel, with the elongation at break rising from 1556% to 1950%. Meanwhile, GO promotes the transportation of electrolyte ions, which are favorable for enhancing the ionic conductivity of the PAA hydrogel. As a result, the assembled supercapacitor based on PAA/GO composite hydrogel electrolyte shows enhanced capacitance retention of 64.3% at a large current density of 20 A g⁻¹ and excellent cycling stability over 10,000 cycles at 5 A g⁻¹. Furthermore, the fabricated flexible supercapacitor devices could maintain outstanding electrochemical performance at various bending angles of 0–90°, indicating a promising prospect for the PAA/GO hydrogel electrolyte in flexible wearable fields.

Keywords: hydrogel electrolyte; supercapacitor; polyacrylic acid (PAA); graphene oxide (GO); flexible



Citation: Xin, Y.; Yu, Z.; Soomro, R.A.; Sun, N. Facile Synthesis of Polyacrylic Acid/Graphene Oxide Composite Hydrogel Electrolyte for High-Performance Flexible Supercapacitors. *Coatings* **2023**, *13*, 382. <https://doi.org/10.3390/coatings13020382>

Academic Editor: Mihai Anastasescu

Received: 10 January 2023

Revised: 27 January 2023

Accepted: 1 February 2023

Published: 7 February 2023



Copyright: © 2023 by the authors. Licensee MDPI, Basel, Switzerland. This article is an open access article distributed under the terms and conditions of the Creative Commons Attribution (CC BY) license (<https://creativecommons.org/licenses/by/4.0/>).

1. Introduction

A supercapacitor is a kind of energy storage device with the highlighted advantages of high power density and a long cycle life [1–4]. With the development and popularization of smart wearable devices, flexible energy storage devices have gradually become a research hotspot [5–7]. Flexible supercapacitors are composed of flexible electrodes and electrolytes. Among them, the flexible electrolyte can not only transport ions but also play the role of separator, thus simplifying the structure of supercapacitors. However, the present electrochemical performance of flexible supercapacitors is still far from satisfactory. The key to realizing excellent electrochemical performance for flexible supercapacitor devices is designing flexible electrodes and electrolytes with excellent electrochemical and mechanical properties [8]. Flexible electrolytes can avoid electrolyte leaks and keep the role of transporting ions under severe deformation. Compared to traditional energy storage devices using liquid electrolytes, devices based on solid electrolytes are safer, stable and variable in shape, which will bring bright prospects for wearable electronic devices in the future [9].

There are three types of common solid electrolytes: ceramic electrolytes [10], gel electrolytes [11] and polyelectrolytes [12]. Among these solid electrolytes, gel polymer electrolytes are considered the ideal ones that have the advantages of high ionic conductivity, low electronic conductivity, suitable mechanical properties, high stability and easy processability [13,14]. Polyacrylic acid hydrogel is a common gel electrolyte for supercapacitors with relatively high ionic conductivity, good hydrophilicity, nontoxicity and low price [15–20]. However, the mechanical property of polyacrylic acid-based gel usually cannot satisfy the requirement of flexible supercapacitors.

Various strategies, including copolymerization, double crosslinking networks, and doping, have been proposed to improve the mechanical strength of polyacrylic acid-based gel electrolytes without sacrificing ionic conductivity. For example, Liao et al. [18] prepared a hydrogel electrolyte with considerable ionic transportation and a noticeable stress response by copolymerizing PAA and octadecyl methacrylate in a vinyl-treated sponge. The polymer chains were grafted onto the 3D interconnected sponge and built a physical framework, thus exhibiting excellent mechanical properties. Huang et al. [21] prepared a new electrolyte by combining polyacrylic acid and vinyl hybrid silica nanoparticles, and the obtained double crosslinking hydrolyte electrolyte could be stretched over 3700% without any cracks. Additives have also been adopted to improve the conductivity and mechanical properties of polyacrylic acid gel. Guo et al. [22] reported Fe^{3+} crosslinked PAA hydrogel electrolyte by adding FeCl_3 into an AA monomer during the polymerization process. The ionic bond between Fe^{3+} and carboxylic acid ions, as well as the intra- and intermolecular hydrogen bonding, endow the supramolecular hydrogel with excellent mechanical properties (extensibility > 700% and stress > 400 kPa). Graphene oxide (GO) has been widely applied in advanced electrochemical devices [23–26]. The surface polar groups and conjugate structure of GO can efficiently promote the transportation of electrolyte ions; therefore, GO is regarded as an excellent ionic conductive additive to the polymer matrix [27–31].

In this study, PAA/GO composite hydrogel electrolytes were successfully prepared by incorporating GO during the polymerization of the AA monomer, as illustrated in Figure 1a. As the abundant surface groups on GO can attract protons and propagate through hydrogen-bonding networks, the transport distance of ions in the gel is greatly shortened with the improvement of ionic conductivity (Figure 1b). Moreover, the oxygen-containing functional groups of GO can crosslink and form hydrogen bonds with the COOH group on the PAA molecular chain, thus improving the mechanical properties of the gel electrolyte. Therefore, compared with pristine PAA gel, the obtained PAA/GO hydrogel electrolytes realize better electrochemical and mechanical properties. After being coupled with commercial active carbon electrodes, the assembled supercapacitor using an optimum PAA/0.5%GO gel electrolyte exhibits excellent electrochemical performance with a high capacitance retention of 64.3% at an enhanced current density of 20 A g^{-1} and outstanding cycling stability with no capacity decay over 10,000 cycles.

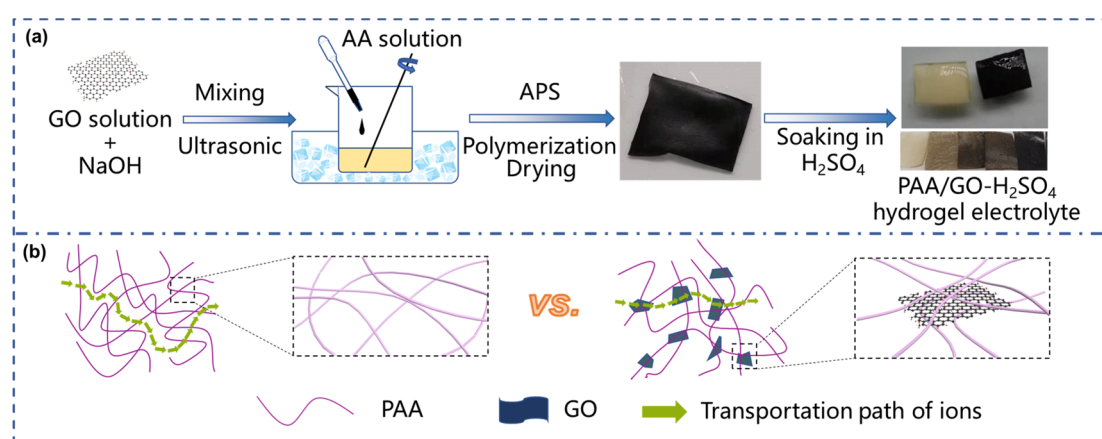


Figure 1. (a) Preparation process of PAA/GO composite gel electrolyte and (b) the schematic diagram for the role of GO in PAA/GO composite gel electrolyte.

2. Experimental

2.1. Materials Synthesis

Graphene oxide (GO) was prepared by the modified Hummer's method [32]. The preparation process of PAA/GO hydrogel electrolyte is shown in Figure 1. First, NaOH

powder was slowly added to GO aqueous solution with a concentration of 10 mg mL^{-1} followed by stirring and ultrasonic treatment. 3 g of acrylic acid (AA) monomer was dispersed in 2 mL water and stirred for 10 min in an ice bath. GO/NaOH solution was added to the acrylic acid solution slowly to control the polymerization speed, and then 0.048 g ammonium persulfate (APS) as initiator was introduced and stirred for 15 min. The obtained AA/GO dispersion was injected into a mold and placed in an oven at a constant temperature of $40 \text{ }^\circ\text{C}$ for 40 h. After polymerization, the polyacrylic acid gel was cut into the desired shape and dried at $90 \text{ }^\circ\text{C}$ for 90 min. Finally, the PAA/GO gel electrolyte was prepared after being soaked in 3 M H_2SO_4 and further removing bubbles in the vacuum dryer. Gel electrolytes with different amounts of GO (0, 0.1 wt%, 0.5 wt%, 1 wt%, 2 wt%) were prepared and named PAA, PAA/0.1%GO, PAA/0.5%GO, PAA/1%GO, PAA/2%GO.

2.2. Materials Characterization

A scanning electron microscope (SEM, HITACHI S480) was used to observe the surface morphology of the gel electrolyte. Fourier transform infrared spectroscopy (FTIR) was measured by a Nicolet 6700 spectrometer. X-ray photoelectron spectroscopy (XPS) was tested using ESCALAB 250. The tensile properties of hydrogels were measured by the electronic universal testing machine CMT6103. The test conditions were as follows: $25 \text{ }^\circ\text{C}$, sample with a size of $3 \text{ cm} \times 2 \text{ cm} \times 0.5 \text{ mm}$, and crosshead speed of 100 mm/min .

2.3. Electrochemical Measurements

All the electrochemical tests of the obtained gel electrolyte were based on the commercial activated carbon (YP50, Kuraray Co., Ltd.) electrode, which was prepared by mixing the activated carbon, acetylene black with polytetrafluoroethylene (PTFE) binder with a mass ratio of 85:10:5 in ethanol. The slurry was dried, rolled into uniform sheets, and cut into round slices with a diameter of 5 mm. After being dried at $120 \text{ }^\circ\text{C}$ for 6 h in a vacuum oven, the electrodes were obtained with an active material loading of 6 mg cm^{-2} . For the assembly of a solid-state supercapacitor, PAA/GO- H_2SO_4 hydrogel electrolytes were cut into a round slice with a diameter of 8 mm. YP50 was used as the working electrode and counter electrode, and Ag/AgCl was used as a reference electrode. The tests were carried out in a three-electrode system, and the operation potential range was set in the range of 0–0.9 V. For the assembly of a flexible supercapacitor, the gel electrolytes and electrodes were cut into $1.5 \text{ cm} \times 2 \text{ cm}$ rectangle slices, with carbon cloth as the flexible current collector. The galvanostatic charge/discharge test was conducted on an Arbin Supercapacitor Test System (BT-G). The cyclic voltammetry (CV) curve and electrochemical impedance spectrum (EIS), with frequencies ranging from 10 mHz to 100 kHz, were measured on the CHI1100C (Chenhua) electrochemical workstation.

3. Results and Discussion

The appearance of the PAA hydrogel is light yellow and transparent (Figure 1), while that of PAA/GO composite gel gets black, and the color gradually deepens with the increase of GO content. The TEM images in Figure A1 show that GO sheets are 5–8 μm in lateral size. The uniform apparent color of PAA/GO gel suggests the homogeneous mixing of PAA and GO nanosheets. Figure 2a–d shows the scanning electron microscopy (SEM) images of PAA and PAA/GO gel with different GO contents. When the GO content is low, the surface of the PAA/GO gel is smooth and flat, which is favorable for electrolytes to fully contact the electrodes. However, when the content of GO increases to 2%, obvious wrinkles appear due to the aggregation of GO layers, which greatly affects the uniformity of gel electrolytes. As shown in Figure 2e,f, the PAA/GO gel can endure bending and torsion well, demonstrating its excellent mechanical strength.

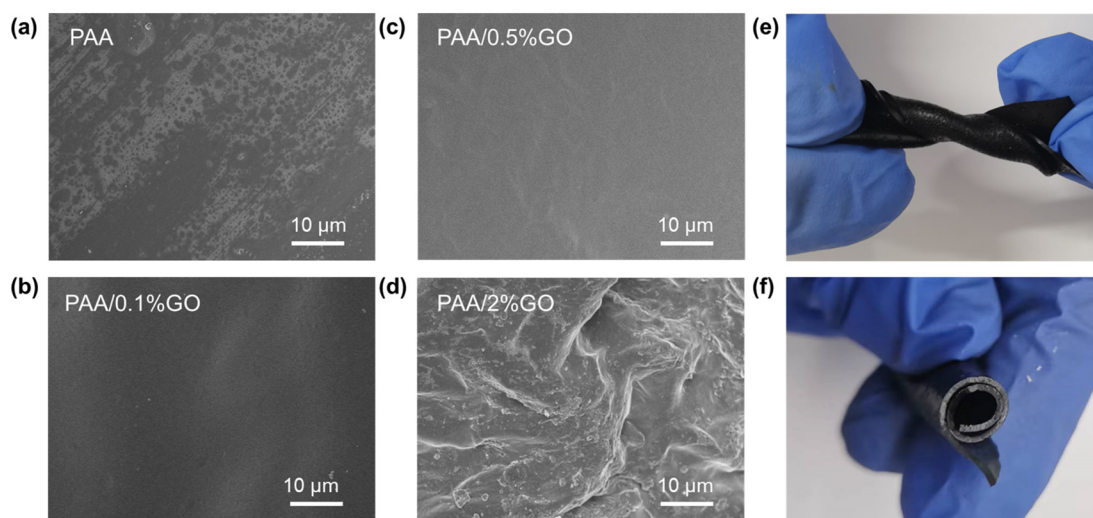


Figure 2. Scanning electron microscope (SEM) images of (a) PAA, (b) PAA/0.1%GO, (c) PAA/0.5%GO, and (d) PAA/2%GO. (e) Torsion properties and (f) rolling properties of composite PAA/0.5%GO electrolytes.

Since the oxygen-containing functional groups of GO can interact with the COOH of polyacrylic chains, GO acts as an effective crosslinking agent in PAA gel, significantly improving the tensile strength of PAA/GO composite gel. The hydrogel can produce large elastic deformation and quickly return to its original shape, as shown in Figure 3a. Figure 3b presents the stress-strain curve of PAA and PAA/0.5%GO, and the tensile strength increases from 4.0 MPa for PAA to 6.1 MPa for PAA/GO composite gel, with elongation at break enhancing from 1556% to 1950%, demonstrating that the addition of GO significantly improved the mechanical properties of PAA gel. The comparison with previously reported polymer electrolytes in Table A1 also verifies the prominent advantage of PAA/GO gel electrolyte.

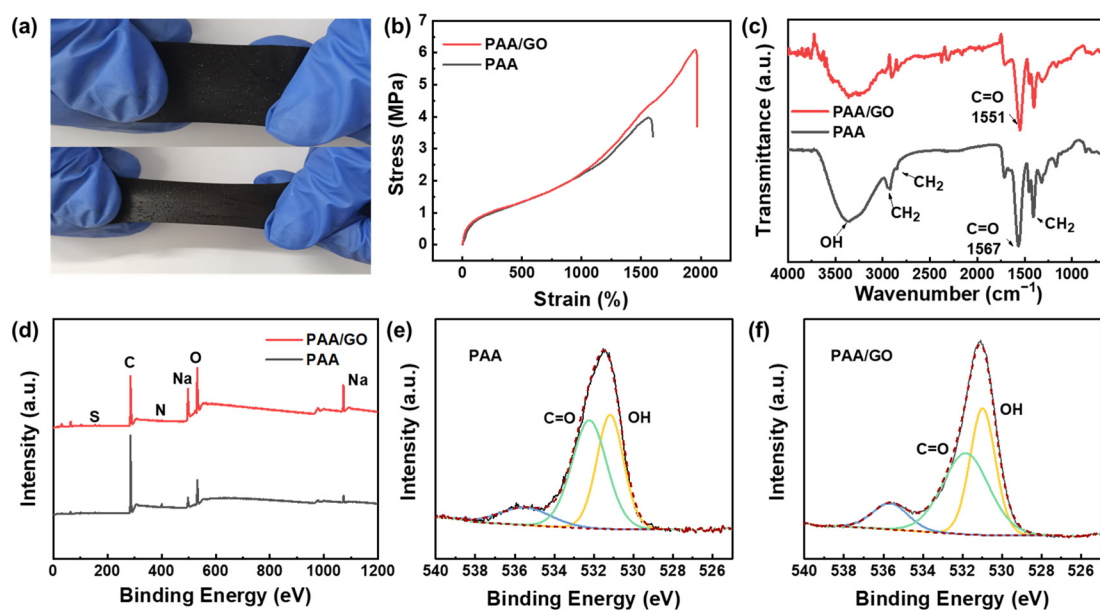


Figure 3. (a) Tensile performance of PAA/0.5%GO composite gel electrolyte. (b) Tensile stress-strain curve comparison of the PAA and PAA/0.5%GO composite gel electrolyte. (c) FTIR and (d) XPS full spectrum of PAA and PAA/0.5%GO. O1s peak fitting of (e) PAA and (f) PAA/GO.

Figure 3c shows the Fourier transform infrared spectroscopy (FTIR) of PAA and PAA/GO hydrogel, where the broad peak at 3360 cm^{-1} is related to the OH stretching vibration. The bending and stretching vibration of CH_2 on the polyacrylic acid molecular chain was observed at 1412 cm^{-1} , 2936 cm^{-1} , and 2847 cm^{-1} [33]. The typical bending vibration of $\text{C}=\text{O}$ in PAA gel appears at 1567 cm^{-1} , while the peak of PAA/GO shifts to 1551 cm^{-1} , which may be ascribed to the influence of GO, which changes the microstructure of PAA gel [34].

XPS was performed to further analyze the elemental composition and content of the PAA gel and PAA/GO gel, as shown in Figure 3d. The PAA and PAA/GO gel are mainly composed of C, O and Na elements, with a minor amount of S and N, which results from the initiator APS. Due to the abundant oxygen-containing groups in GO, the PAA/GO gel displays a relatively higher O content than the pristine PAA gel [34]. Peak fitting of O1s was conducted to further determine the specific functional groups' types in the PAA and PAA/GO gels, as shown in Figure 3e,f. The O1s can be deconvoluted into OH, $\text{C}=\text{O}$ and adsorbed H_2O species located at 531 eV, 532.5 eV and 536 eV, respectively [35–37]. Compared with PAA, the PAA/GO gel shows a decreased proportion of $\text{C}=\text{O}$ and enhanced OH functional groups due to the addition of GO, which not only facilitates crosslinking with the COOH of PAA but also helps the transportation of electrolyte ions, thus improving the conductivity of gel electrolytes.

Ionic conductivity plays an essential role in determining the electrochemical performance of solid electrolytes. Figure 4a shows the Nyquist plots of PAA/GO electrolytes with different GO contents, and the intersection points of the oblique lines with the X-axis are usually considered intrinsic resistance of the ion gel, as the ohmic resistance of the testing device is negligible. The ionic conductivity was calculated according to formula $\rho = L/RS$, where L is the thickness, R is the resistance of gel and S is the geometric area of the electrode/electrolyte interface [38,39]. With the increase of GO content, the conductivity value of PAA/GO electrolyte steadily rises due to the transportation effect of oxygenic groups on ions, and the introduction of GO significantly shortens the ion transport path and thus reduces the internal resistance of gel electrolyte. The conductivity reaches the highest when the GO content is 0.5%, as displayed in Figure 4b. Further increasing the proportion of GO, the conductivity of PAA/GO electrolyte gradually decreases because GO nanosheet aggregation hinders ion transportation.

The electrochemical performance of the obtained PAA/GO gel electrolyte was evaluated by assembling supercapacitors with commercial active carbon as electrodes and the PAA/GO gel as electrolyte. Figure 4c,d compares the CV curves of PAA and PAA/0.5%GO electrolyte at various scan rates ranging from 10 mV s^{-1} to 200 mV s^{-1} . The curve shapes of PAA and PAA/0.5%GO are similar to a rectangle, and the pseudocapacitance peaks at about 0.4 V can mainly be attributed to the contribution from PAA [40]. With the increase in scan rate, the shape of the CV curve gradually becomes a flat shuttle. However, PAA/0.5%GO could still maintain a larger area than PAA, indicating that PAA/0.5%GO's better rate performance and maintained electrochemical double-layer capacitance behavior even at high scan rates. The capacitive contribution at different scan rates for the electrode using PAA/0.5%GO electrolyte was further quantitatively determined according to Dunn's method [41], as shown in Figure A2. With the increase in scan rates from 2 mV s^{-1} to 50 mV s^{-1} , the electrochemical double layer capacitance ratio rises from 71.4% to 92.1%. Figure 4e,f show the charge–discharge curves under different current densities of the assembled supercapacitors using PAA/0.5%GO gel electrolyte. The highly symmetrical charge–discharge curves with no obvious IR drop, even under a high current density of 20 A g^{-1} , suggest the small internal resistance and good ionic conductivity of the PAA/GO gel electrolyte. The specific capacitance of the supercapacitors using the PAA/GO gel electrolyte with different GO contents was calculated based on the charge–discharge curve, and similar specific capacitance values were observed at a small current density of 0.2 A g^{-1} for the PAA/GO gel electrolyte and the conventional PAA gel electrolyte, as shown in Figure 4g. The superiority of PAA/GO gel electrolyte becomes prominent

with the increased current densities. The specific capacitance can maintain 127 F g^{-1} for PAA/0.5%GO when the current density rises to 20 A g^{-1} , much higher than 53 F g^{-1} for the PAA electrolyte. Compared to the capacitance value at 0.2 A g^{-1} , the capacitance retention for PAA/0.5%GO at an increased current density of 20 A g^{-1} is as high as 64.3%, further verifying the favorable effect of GO on the improvement of rapid ion transportation. Here, the comparatively good capacitance retention of PAA/0.5%GO than PAA/1%GO at a large current density of 20 A g^{-1} may be mainly ascribed to the higher conductivity of the gel electrolytes. In order to examine the long-term cycling stability of the gel electrolyte, the supercapacitor using PAA/0.5%GO gel electrolyte was galvanostatically charged-discharged at a current density of 5 A g^{-1} (Figure 4h). The capacity retention over 10,000 cycles is as high as 103.6%, demonstrating that the gel electrolyte has excellent cycle stability and great application potential. From the charge-discharge curves of the first ten cycles and the last ten cycles, it can be found that the charge-discharge behavior is consistent with isosceles triangle shapes and no obvious voltage drops, further proving the excellent electrochemical stability of PAA/GO gel electrolyte in the long-term charge-discharge cycling process.

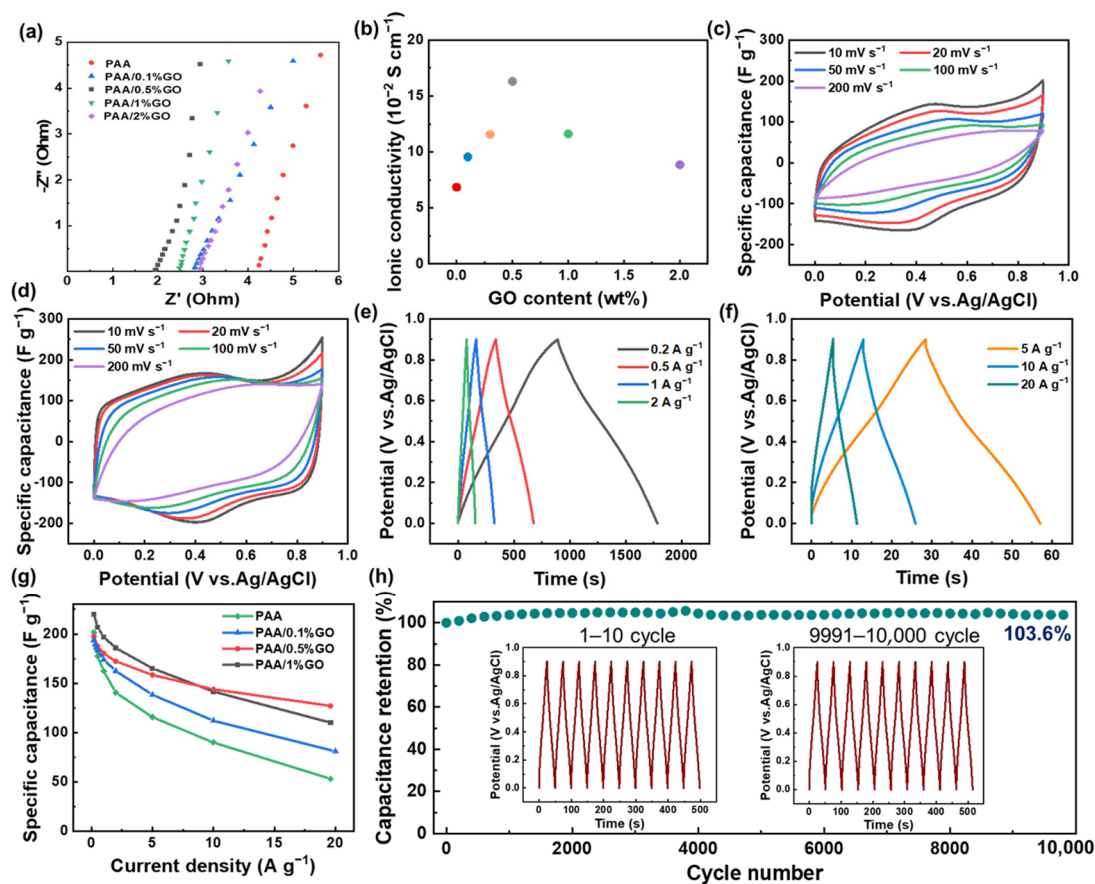


Figure 4. (a) Nyquist plots of PAA/GO electrolytes with different GO contents. (b) Ionic conductivity varies according to GO content. CV curves of the (c) PAA and (d) PAA/0.5%GO solid supercapacitor in 3 M H₂SO₄. (e,f) Galvanostatic charge-discharge curves at different current densities. (g) Specific capacitances as a function of current densities. (h) The cycling stability of PAA/0.5%GO at 5 A g^{-1} for 10,000 cycles.

To further investigate the practical application prospect of the PAA/GO gel electrolyte in flexible supercapacitors, carbon cloth was used as the current collector, with YP50F as electrode material, PAA/0.5%GO as the gel electrolyte and plastic as external packaging to assemble the packaged supercapacitor device. As shown in Figure 5a, the supercapacitor demonstrates excellent flexibility under various bending conditions (0° , 30° , 60° and 90°). Furthermore, three supercapacitors were connected in series and wrapped around the wrist

to simulate the practical application of flexible wearable devices, and it was found that the little bulb could be well lit (Figure 5b), indicating the potential application prospects of the flexible supercapacitor with PAA/0.5%GO as the gel electrolyte.

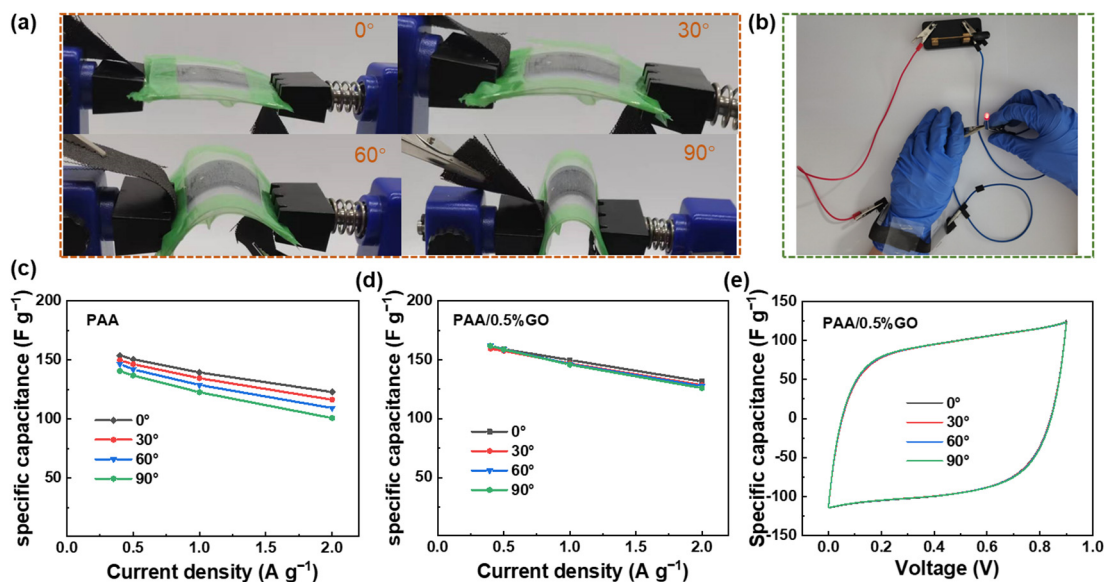


Figure 5. (a) Digital photographs of flexible supercapacitor tested at various bending angles of 0°, 30°, 60° and 90°. (b) Digital display of a small bulb lighted by three flexible supercapacitors connected in series. Rate performance for (c) PAA and (d) PAA/0.5%GO gel electrolyte at different bending angles. (e) CV curves at a scanning rate of 50 mV s⁻¹ for PAA/0.5%GO gel electrolyte at different bending angles.

Figure 5c,d compares the bending performance of PAA and PAA/0.5%GO hydrogel electrolyte. For PAA gel, with the increase of bending angle, both capacitance and rate performance decline dramatically, which can be ascribed to insufficient contact between the electrode and the electrolyte under bending conditions that affect the diffusion of electrolyte ions. While for PAA/0.5%GO gel, little change can be observed in the rate curves at four different angles, further proving the excellent bending performance of PAA/0.5%GO hydrogel. Figure 5e shows the CV curve of PAA/0.5%GO at a scanning rate of 50 mV s⁻¹ under various bending conditions. The coincident rectangular curves indicate that the flexible supercapacitor can still maintain double-layer capacitive behavior in the bending state with outstanding capacitance performance.

4. Conclusions

In summary, we successfully fabricated high-performance PAA/GO composite hydrogel electrolytes for flexible supercapacitors. The effective crosslinking between GO and the PAA polymer chain significantly enhanced the mechanical properties of the gel electrolyte, and the tensile strength increased from 4.0 MPa for PAA to 6.1 MPa for PAA/GO composite gel, with the elongation at break enhancing from 1556% to 1950%. Meanwhile, the addition of GO could improve the ionic conductivity of PAA gel and promote the transportation of electrolyte ions. As a result, the assembled electric double-layer capacitor using an optimum PAA/0.5%GO gel electrolyte exhibits greatly improved electrochemical performance with a high capacitance retention of 64.3% at an enhanced current density of 20 A g⁻¹ and excellent cycling stability over 10,000 cycles at 5 A g⁻¹. Moreover, the fabricated flexible supercapacitor devices can maintain outstanding electrochemical performance at various bending conditions of 0–90°, demonstrating the promising practical application prospects of the PAA/GO electrolyte.

Author Contributions: Conceptualization, Y.X. and N.S.; methodology, Y.X.; validation, Y.X. and Z.Y.; formal analysis, Y.X.; investigation, Y.X.; resources, Y.X. and R.A.S.; data curation, Y.X. and Z.Y.; writing—original draft preparation, Y.X.; writing—review and editing, R.A.S. and N.S.; visualization, Y.X.; supervision, N.S.; project administration, N.S.; funding acquisition, N.S. All authors have read and agreed to the published version of the manuscript.

Funding: This work was financially supported by the Fundamental Research Funds for the Central Universities (buctrc202141).

Institutional Review Board Statement: Not applicable.

Informed Consent Statement: Not applicable.

Data Availability Statement: All data that support the findings of this study are included within the article.

Conflicts of Interest: The authors declare no conflict of interest.

Appendix A

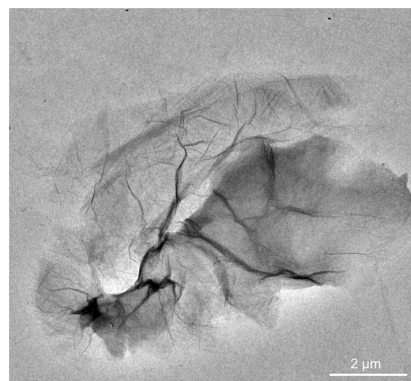


Figure A1. Transmission electron microscope (TEM) image of graphene oxide.

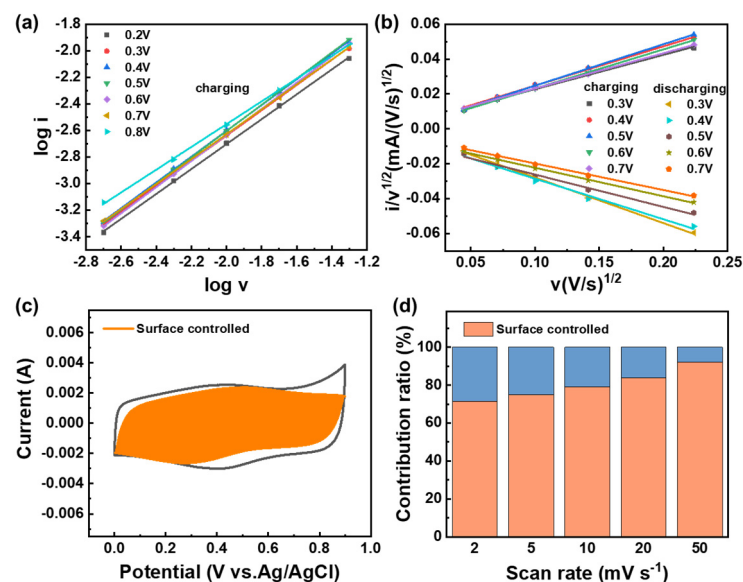


Figure A2. Evaluating the contribution from diffusion controlled and surface-controlled capacitance. (a) Plot of $\log i$ vs. $\log v$ for determining the slope b ; (b) Plot of square root of scan rate ($v^{1/2}$) vs. current/ $v^{1/2}$ ($i/v^{1/2}$) at different potentials during charging and discharging; (c) Contribution from surface-controlled current towards charge storage at 10 mV s $^{-1}$; (d) Contribution ratio of surface-controlled capacitance at different scan rates.

Table A1. Comparison of stress, strain and ionic conductivity of PAA/0.5%GO gel electrolyte in this work with the polymer electrolytes reported in recent works.

	Stress (MPa)	Strain (%)	Ionic Conductivity ($10^{-2} \text{ S cm}^{-1}$)	Reference
S-PAA	2.2	1100%	1.5	[18]
VSNPs-PAA	0.12	3700%	0.75	[21]
Fe ³⁺ /PAA	0.4	700%	9	[22]
Li-AG/PAM DN	1.1	2780%	4.1	[42]
BC-reinforced PAM	0.33	1300%	12.5	[43]
PK10 AGPE	2.22	1243%	21	[44]
B-PVA/KCl/GO	\	\	4.75	[45]
PAA/GO	6.1	1950%	16.81	This work

References

- Zhang, J.; Luo, J.; Guo, Z.; Liu, Z.; Duan, C.; Dou, S.; Yuan, Q.; Liu, P.; Ji, K.; Zeng, C.; et al. Ultrafast Manufacturing of Ultrafine Structure to Achieve An Energy Density of Over 120 Wh kg⁻¹ in Supercapacitors. *Adv. Energy Mater.* **2022**, *27*, 2203061. [CrossRef]
- Muralee Gopi, C.V.V.; Vinodh, R.; Sambasivam, S.; Obaidat, I.M.; Kim, H.-J. Recent progress of advanced energy storage materials for flexible and wearable supercapacitor: From design and development to applications. *J. Energy Storage* **2020**, *27*, 101035. [CrossRef]
- Xiao, J.; Han, J.; Zhang, C.; Ling, G.; Kang, F.; Yang, Q.H. Dimensionality, Function and Performance of Carbon Materials in Energy Storage Devices. *Adv. Energy Mater.* **2021**, *12*, 2100775. [CrossRef]
- Yu, S.; Sun, N.; Hu, L.; Wang, L.; Zhu, Q.; Guan, Y.; Xu, B. Self-template and self-activation synthesis of nitrogen-doped hierarchical porous carbon for supercapacitors. *J. Power Source* **2018**, *405*, 132–141. [CrossRef]
- Wang, Y.; Wu, X.; Han, Y.; Li, T. Flexible supercapacitor: Overview and outlooks. *J. Energy Storage* **2021**, *42*, 103053. [CrossRef]
- Thomas, S.A.; Patra, A.; Al-Shehri, B.M.; Selvaraj, M.; Aravind, A.; Rout, C.S. MXene based hybrid materials for supercapacitors: Recent developments and future perspectives. *J. Energy Storage* **2022**, *55*, 105765. [CrossRef]
- Swain, N.; Tripathy, A.; Thirumurugan, A.; Saravanakumar, B.; Schmidt-Mende, L.; Ramadoss, A. A brief review on stretchable, compressible, and deformable supercapacitor for smart devices. *Chem. Eng. J.* **2022**, *446*, 136876. [CrossRef]
- Dubal, D.P.; Chodankar, N.R.; Kim, D.H.; Gomez-Romero, P. Towards flexible solid-state supercapacitors for smart and wearable electronics. *Chem. Soc. Rev.* **2018**, *47*, 2065–2129. [CrossRef]
- Ma, G.; Dong, M.; Sun, K.; Feng, E.; Peng, H.; Lei, Z. A redox mediator doped gel polymer as an electrolyte and separator for a high performance solid state supercapacitor. *J. Mater. Chem. A* **2015**, *3*, 4035–4041. [CrossRef]
- Menkin, S.; Lifshitz, M.; Haimovich, A.; Goor, M.; Blanga, R.; Greenbaum, S.G.; Goldbourt, A.; Golodnitsky, D. Evaluation of ion-transport in composite polymer-in-ceramic electrolytes. Case study of active and inert ceramics. *Electrochim. Acta* **2019**, *304*, 447–455. [CrossRef]
- Liu, S.; Zhong, Y.; Zhang, X.; Pi, M.; Wang, X.; Zhu, R.; Cui, W.; Ran, R. Highly Deformable, Conductive Double-Network Hydrogel Electrolytes for Durable and Flexible Supercapacitors. *ACS Appl. Mater. Interfaces* **2022**, *14*, 15641–15652. [CrossRef]
- Luangaramvej, P.; Dubas, S.T. Two-step polyaniline loading in polyelectrolyte complex membranes for improved pseudo-capacitor electrodes. *e-Polymers* **2021**, *21*, 194–199. [CrossRef]
- Na, R.; Huo, P.; Zhang, X.; Zhang, S.; Du, Y.; Zhu, K.; Lu, Y.; Zhang, M.; Luan, J.; Wang, G. A flexible solid-state supercapacitor based on a poly(aryl ether ketone)-poly(ethylene glycol) copolymer solid polymer electrolyte for high temperature applications. *RSC Adv.* **2016**, *6*, 65186–65195. [CrossRef]
- Alipoori, S.; Mazinani, S.; Aboutalebi, S.H.; Sharif, F. Review of PVA-based gel polymer electrolytes in flexible solid-state supercapacitors: Opportunities and challenges. *J. Energy Storage* **2020**, *27*, 101072. [CrossRef]
- Chan, C.Y.; Wang, Z.; Jia, H.; Ng, P.F.; Chow, L.; Fei, B. Recent advances of hydrogel electrolytes in flexible energy storage devices. *J. Mater. Chem. A* **2021**, *9*, 2043–2069. [CrossRef]
- Hu, M.; Wang, J.; Liu, J.; Zhang, J.; Ma, X.; Huang, Y. An intrinsically compressible and stretchable all-in-one configured supercapacitor. *ChemComm* **2018**, *54*, 6200–6203. [CrossRef]
- Zhang, X.; Pei, Z.; Wang, C.; Yuan, Z.; Wei, L.; Pan, Y.; Mahmood, A.; Shao, Q.; Chen, Y. Flexible Zinc-Ion Hybrid Fiber Capacitors with Ultrahigh Energy Density and Long Cycling Life for Wearable Electronics. *Small* **2019**, *15*, 1903817. [CrossRef]
- Liao, H.; Zhou, F.; Zhang, Z.; Yang, J. A self-healable and mechanical toughness flexible supercapacitor based on polyacrylic acid hydrogel electrolyte. *Chem. Eng. J.* **2019**, *357*, 428–434. [CrossRef]
- Abubshait, H.A.; Saad, M.; Iqbal, S.; Abubshait, S.A.; Bahadur, A.; Raheel, M.; Alshammari, F.H.; Alwadai, N.; Alrbyawi, H.; Abourehab, M.A.S.; et al. Co-doped zinc oxide nanoparticles embedded in Polyvinylalcohol Hydrogel as solar light derived photocatalyst disinfection and removal of coloured pollutants. *J. Mol. Struct.* **2023**, *1271*, 134100. [CrossRef]

20. Iqbal, S.; Javed, M.; Qamar, M.A.; Bahadur, A.; Fayyaz, M.; Akbar, A.; Alsaab, H.O.; Awwad, N.S.; Ibrahim, H.A. Synthesis of Cu-ZnO/Polyacrylic Acid Hydrogel as Visible-Light-Driven Photocatalyst for Organic Pollutant Degradation. *ChemistrySelect* **2022**, *7*, e202103694. [[CrossRef](#)]
21. Huang, Y.; Zhong, M.; Huang, Y.; Zhu, M.; Pei, Z.; Wang, Z.; Xue, Q.; Xie, X.; Zhi, C. A self-healable and highly stretchable supercapacitor based on a dual crosslinked polyelectrolyte. *Nat. Commun.* **2015**, *6*, 10310. [[CrossRef](#)] [[PubMed](#)]
22. Guo, Y.; Zhou, X.; Tang, Q.; Bao, H.; Wang, G.; Saha, P. A self-healable and easily recyclable supramolecular hydrogel electrolyte for flexible supercapacitors. *J. Mater. Chem. A* **2016**, *4*, 8769–8776. [[CrossRef](#)]
23. Cao, Y.-C.; Xu, C.; Wu, X.; Wang, X.; Xing, L.; Scott, K. A poly (ethylene oxide)/graphene oxide electrolyte membrane for low temperature polymer fuel cells. *J. Power Source* **2011**, *196*, 8377–8382. [[CrossRef](#)]
24. Huang, Y.-F.; Wu, P.-F.; Zhang, M.-Q.; Ruan, W.-H.; Giannelis, E.P. Boron cross-linked graphene oxide/polyvinyl alcohol nanocomposite gel electrolyte for flexible solid-state electric double layer capacitor with high performance. *Electrochim. Acta* **2014**, *132*, 103–111. [[CrossRef](#)]
25. Xu, B.; Wang, H.; Zhu, Q.; Sun, N.; Anasori, B.; Hu, L.; Wang, F.; Guan, Y.; Gogotsi, Y. Reduced graphene oxide as a multi-functional conductive binder for supercapacitor electrodes. *Energy Storage Mater.* **2018**, *12*, 128–136. [[CrossRef](#)]
26. Sun, N.; Guan, Y.; Liu, Y.-T.; Zhu, Q.; Shen, J.; Liu, H.; Zhou, S.; Xu, B. Facile synthesis of free-standing, flexible hard carbon anode for high-performance sodium ion batteries using graphene as a multi-functional binder. *Carbon* **2018**, *137*, 475–483. [[CrossRef](#)]
27. Stankovich, S.; Dikin, D.A.; Piner, R.D.; Kohlhaas, K.A.; Kleinhammes, A.; Jia, Y.; Wu, Y.; Nguyen, S.T.; Ruoff, R.S. Synthesis of graphene-based nanosheets via chemical reduction of exfoliated graphite oxide. *Carbon* **2007**, *45*, 1558–1565. [[CrossRef](#)]
28. Zhu, Y.; Murali, S.; Cai, W.; Li, X.; Suk, J.W.; Potts, J.R.; Ruoff, R.S. Graphene and graphene oxide: Synthesis, properties, and applications. *Adv. Mater.* **2010**, *22*, 3906–3924. [[CrossRef](#)]
29. Huang, Y.; Zhu, M.; Huang, Y.; Pei, Z.; Li, H.; Wang, Z.; Xue, Q.; Zhi, C. Multifunctional Energy Storage and Conversion Devices. *Adv. Mater.* **2016**, *28*, 8344–8364. [[CrossRef](#)]
30. Pan, C.; Liu, L.; Gai, G. Recent Progress of Graphene-Containing Polymer Hydrogels: Preparations, Properties, and Applications. *Macromol. Mater. Eng.* **2017**, *302*, 1700184. [[CrossRef](#)]
31. Tian, Y.; Yu, Z.; Cao, L.; Zhang, X.L.; Sun, C.; Wang, D.-W. Graphene oxide: An emerging electromaterial for energy storage and conversion. *J. Energy Chem.* **2021**, *55*, 323–344. [[CrossRef](#)]
32. Marcano, D.C.; Kosynkin, D.V.; Berlin, J.M.; Sinititskii, A.; Sun, Z.; Slesarev, A.; Alemany, L.B.; Lu, W.; Tour, J.M. Improved Synthesis of Graphene Oxide. *ACS Nano* **2010**, *4*, 4806–4814. [[CrossRef](#)]
33. Han, Q.; Chen, L.; Li, W.; Zhou, Z.; Fang, Z.; Xu, Z.; Qian, X. Self-assembled three-dimensional double network graphene oxide/polyacrylic acid hybrid aerogel for removal of Cu(2+) from aqueous solution. *Environ. Sci. Pollut. Res.* **2018**, *25*, 34438–34447. [[CrossRef](#)]
34. Al-Gaashani, R.; Najjar, A.; Zakaria, Y.; Mansour, S.; Atieh, M.A. XPS and structural studies of high quality graphene oxide and reduced graphene oxide prepared by different chemical oxidation methods. *Ceram. Int.* **2019**, *45*, 14439–14448. [[CrossRef](#)]
35. Piloto, C.; Shafiei, M.; Khan, H.; Gupta, B.; Tesfamichael, T.; Motta, N. Sensing performance of reduced graphene oxide-Fe doped WO₃ hybrids to NO₂ and humidity at room temperature. *Appl. Surf. Sci.* **2018**, *434*, 126–133. [[CrossRef](#)]
36. Kong, W.; Yue, Q.; Li, Q.; Gao, B. Adsorption of Cd(2+) on GO/PAA hydrogel and preliminary recycle to GO/PAA-CdS as efficient photocatalyst. *Sci. Total Environ.* **2019**, *668*, 1165–1174. [[CrossRef](#)]
37. Feng, Z.; Feng, C.; Chen, N.; Lu, W.; Wang, S. Preparation of composite hydrogel with high mechanical strength and reusability for removal of Cu(II) and Pb(II) from water. *Sep. Purif. Technol.* **2022**, *300*, 121894. [[CrossRef](#)]
38. Wang, S.H.; Hou, S.S.; Kuo, P.L.; Teng, H. Poly(ethylene oxide)-co-poly(propylene oxide)-based gel electrolyte with high ionic conductivity and mechanical integrity for lithium-ion batteries. *ACS Appl. Mater. Interfaces* **2013**, *5*, 8477–8485. [[CrossRef](#)]
39. Yang, X.; Zhang, F.; Zhang, L.; Zhang, T.; Huang, Y.; Chen, Y. A High-Performance Graphene Oxide-Doped Ion Gel as Gel Polymer Electrolyte for All-Solid-State Supercapacitor Applications. *Adv. Funct. Mater.* **2013**, *23*, 3353–3360. [[CrossRef](#)]
40. Fan, X.; Lu, Y.; Xu, H.; Kong, X.; Wang, J. Reversible redox reaction on the oxygen-containing functional groups of an electrochemically modified graphite electrode for the pseudo-capacitance. *J. Mater. Chem.* **2011**, *21*, 18753. [[CrossRef](#)]
41. Islam, T.; Hasan, M.M.; Shah, S.S.; Karim, M.R.; Al-Mubaddel, F.S.; Zahir, M.H.; Dar, M.A.; Hossain, M.D.; Aziz, M.A.; Ahammad, A.J.S. High yield activated porous coal carbon nanosheets from Boropukuria coal mine as supercapacitor material: Investigation of the charge storing mechanism at the interfacial region. *J. Energy Storage* **2020**, *32*, 101908. [[CrossRef](#)]
42. Lin, T.; Shi, M.; Huang, F.; Peng, J.; Bai, Q.; Li, J.; Zhai, M. One-Pot Synthesis of a Double-Network Hydrogel Electrolyte with Extraordinarily Excellent Mechanical Properties for a Highly Compressible and Bendable Flexible Supercapacitor. *ACS Appl. Mater. Interfaces* **2018**, *10*, 29684–29693. [[CrossRef](#)] [[PubMed](#)]
43. Li, X.; Yuan, L.; Liu, R.; He, H.; Hao, J.; Lu, Y.; Wang, Y.; Liang, G.; Yuan, G.; Guo, Z. Engineering Textile Electrode and Bacterial Cellulose Nanofiber Reinforced Hydrogel Electrolyte to Enable High-Performance Flexible All-Solid-State Supercapacitors. *Adv. Energy Mater.* **2021**, *11*, 2003010. [[CrossRef](#)]

44. Hu, X.; Fan, L.; Qin, G.; Shen, Z.; Chen, J.; Wang, M.; Yang, J.; Chen, Q. Flexible and low temperature resistant double network alkaline gel polymer electrolyte with dual-role KOH for supercapacitor. *J. Power Source* **2019**, *414*, 201–209. [[CrossRef](#)]
45. Peng, H.; Lv, Y.; Wei, G.; Zhou, J.; Gao, X.; Sun, K.; Ma, G.; Lei, Z. A flexible and self-healing hydrogel electrolyte for smart supercapacitor. *J. Power Source* **2019**, *431*, 210–219. [[CrossRef](#)]

Disclaimer/Publisher’s Note: The statements, opinions and data contained in all publications are solely those of the individual author(s) and contributor(s) and not of MDPI and/or the editor(s). MDPI and/or the editor(s) disclaim responsibility for any injury to people or property resulting from any ideas, methods, instructions or products referred to in the content.